arXiv:1410.3047v1 [quant-ph] 12 Oct 2014

Single-step transfer or exchange of multipartite quantum entanglement with minimum resources

Chui-Ping Yang[1], Qi-Ping Su[1], Shi-Biao Zheng[2⋆], and Siyuan Han[3,4⋆]

[1]*Department of Physics, Hangzhou Normal University, Hangzhou, Zhejiang 310036, China*

[2]*Department of Physics, Fuzhou University, Fuzhou 350002, China*

[3]*Department of Physics and Astronomy, University of Kansas, Lawrence, Kansas 66045, USA*

[4]*Beijing National Laboratory for Condensed Matter Physics, Institute of Physics, Chinese Academy of Sciences, Beijing 100190, China*

⋆ *Correspondence and requests for materials should be addressed to S.Han (email: han@ku.edu) or S.B.Zheng (sbzheng11@163.com)*

The transfer or exchange of multipartite quantum states is critical to the realization of large-scale quantum information processing and quantum communication. A challenging question in this context is: "What is the minimum resource required and how to simultaneously transfer or exchange multipartite quantum entanglement between two sets of qubits". Finding the answer to these questions is of great importance to quantum information science. In this work, we demonstrate that by using a single quantum two-level system - the simplest quantum object - as a coupler arbitrary multipartite quantum states (either entangled or separable) can be transferred or exchanged simultaneously between two sets of qubits. Our findings offer the potential to significantly reduce the resources needed to construct and operate large-scale quantum information networks consisting of many multi-qubit registers,

memory cells, and processing units.

Entanglement arises from nonclassical correlation between the constituents of multipartite quantum systems. It is one of the most profound and difficult to understand aspects of quantum physics. Entanglement is indispensable in quantum information science as demonstrated by Shor's factorization algorithm [1] and various quantum key distribution protocols [2,3]. Recently, considerable interest has been devoted to the application of entangled states in quantum computation [4,5], quantum cryptography [2,6], teleportation [7-9], and quantum copying [10,11] and many previously unknown or unexpected properties of entanglement, such as entanglement swapping [10] and entanglement sudden death [12], have been discovered. Over the past decade, experimentalists have generated and verified entanglement in a variety of physical systems, including eight photons via linear optical devices [13,14], fourteen trapped ions [15], two atoms in cavity QED [16,17], two excitons in a single quantum dot [18], electron spins in two proximal nitrogen-vacancy centres [19], and up to five superconducting qubits coupled via a single cavity or capacitors [20-25].

Because transfer or exchange of arbitrary multipartite states (TEAMS) is of great importance to utilizing entanglement for quantum information processing (QIP) and quantum communication, it has attracted much attention. In principle, TEAMS can be accomplished by expanding either entanglement-based quantum teleportation protocols or non-teleportation protocols. For instance, many theoretical schemes [26-30] and experiments [31-35] have investigated how to transfer or exchange quantum states between two qubits using *entanglement-based* quantum teleportation protocols [7]. Among experiments, quantum state transfer between two superconducting qubits has been demonstrated in circuits consisting of multiple superconducting qubits coupled to planar resonators [36-39]. Alternatively, quantum state transfer or exchange can also be realized using

non-teleportation protocols. For instance, by using photons (transmitted via an optical fiber) as the information carriers the transfer of quantum states from one atom to another has been explored [40-42]. In addition, a quantum network, with single atoms placed in fiber-connected cavities, has been proposed and the transfer of atomic quantum states and the creation of entanglement between two distant nodes of the network have been demonstrated experimentally [43].

Because in the work mentioned above the states being transferred or exchanged are single particle states, it is not granted that these protocols can be applied to multipartite states without a substantial increase of resources (e.g., multiple EPR pairs). As quantum networks play an increasingly important role in scalable QIP it is imperative to explore new methods to realizing TEAMS with a minimum amount of resources. Some of the most urgent issues in this context include "What is the minimum quantum hardware resource (e.g., the number of qubits and couplers) required to transfer or exchange arbitrary multipartite quantum states between two quantum registers each having N qubits?" and "Given the minimum quantum hardware resource, could transfer or exchange of N-partite states be done with a single step of operation?". Positive answers to these questions would not only have significant impact on the architecture of future quantum networks but also is of highly interesting to the foundation of quantum mechanics.

In this work, we answer these two critical questions by considering a generic model system consisting of $2N$ qubits (e.g., spin $\frac{1}{2}$ particles) coupled to a two-level coupler C (Fig. 1). The $2N$ qubits are divided arbitrarily into two sets, labelled as the set A and set B respectively, each containing N qubits. It is also assumed that qubits in the same set may or may not have direct

intra-set coupling and that no *direct* coupling exists between qubits in different sets. The two-level coupler acts as an intermediary to allow quantum information, in the form of multipartite quantum states, flow from A to B and vice versa. We show that for $N \geq 2$ by multiplexing a *single two-level coupler* is sufficient to generate coupler-mediated effective interaction between the N pairs of qubits and that arbitrary N-partite states can be transferred or exchanged between A and B in a *single* step. Namely, the *minimum* quantum hardware resource to transfer or exchange a piece of N-bit quantum information simultaneously in one step between two sets is a single quantum two-level coupler. In addition, the coupler can also be used to mediate interactions between qubits in the same set, allowing creation and manipulation of entanglement within each set.

This result is nontrivial and not known *a priori* because the Hilbert space of each N-qubit set is 2^N-dimensional whereas that of the coupler is only 2-dimensional, which is the minimum for any quantum systems, and the states to be exchanged or transferred between A and B registers are arbitrary N-partite states (e.g., entangled or separable, pure or mixed). According to conventional wisdoms, one would think that transferring or exchanging quantum information, which requires a 2^N-dimensional Hilbert space to accommodate, between two N-qubit sets in one step via a single coupler would require the coupler also having at least a 2^N-dimensional Hilbert space. Thus, it is natural to think that transferring or exchanging N-qubit states would require N auxiliary two-level coupler (TLC) plus one operational step, or alternatively one TLC plus N repeated operational steps, to accomplish.

We point out that the method proposed here has several distinctive advantages: (i) Only a

two-level coupler is needed, and TEAMS can be performed simultaneously in a single step without the use of classical rf/microwave/optical pulses during the state transfer/exchange operation. This unique feature reduces the complexity of the circuits and operations. (ii) The two-level coupler C can be either a true quantum two-level system (TLS), such as an electron spin, or an effective TLS, such as the two lowest levels of a superconducting qubit, so that the scheme can be applied to a large variety of physical quantum information networks. (iii) During the operation the coupler stays mostly in its ground state so that the effects of quantum channel decoherence is greatly suppressed. This property allows the use of couplers with shorter decoherence time but has other desirable attributes such as rapid frequency tunability, design flexibility, or good scalability. (iv) It offers the flexibility of reconfiguring interactions between pairs of qubits, either intra-set or inter-set, *in situ* to perform various QIP tasks without changing hardware wirings. (v) By connecting the qubits to multiple, e.g., two or three two-level couplers, the structure can be expanded into one- or two-dimensional quantum networks - a promising architecture for scalable QIP.

In what follows, we derive the interaction Hamiltonian that governs the system dynamics of the $2N$ qubits plus one two-level coupler. It is evident from the Hamiltonian that N pairs of *in situ* programmable qubit-qubit superexchange interaction can occur in parallel without interference to each other allowing the possibility of realizing TEAMS in a single step (e.g., by making all coupler-mediated effective pair interactions the same strength). As an example, we describe in detail how to perform N-partite state exchange (swap) and transfer using this generic configuration. Furthermore, we propose a circuit QED-based implementation of the scheme. With realistic device and circuit parameters, numerical simulations show that the fidelity can reach 99.1% for Bell-state

transfer and no less than 96.3% for Bell-state swap. Finally, we summarize the key result and its impact on the future development of quantum information science.

Results

Hamiltonian. Without the loss of generality we consider two sets of otherwise noninteracting qubits connected to a two-level coupler C, hereafter referred to as coupler C for simplicity, as illustrated in Fig. 1(a). The first set contains N qubits $\{a_1, a_2, ...a_j, ...a_N\}$ while the second set contains the remaining N qubits $\{b_1, b_2, ..., b_k, ...b_N\}$. The two logic states of the qubits a_j (b_k) are labelled as $|0\rangle_{a_j(b_k)}$ and $|1\rangle_{a_j(b_k)}$ and that of the coupler C are denoted as $|g\rangle_{\rm c}$ and $|e\rangle_{\rm c}$, respectively. For qubit a_j, we define the operators $\hat{a}_j$ and $\hat{a}_j^+$, which satisfy $\hat{a}_j |0\rangle_{a_j} = 0$, $\hat{a}_j |1\rangle_{a_j} = |0\rangle_{a_j}$, and $\hat{a}_j^+ |0\rangle_{a_j} = |1\rangle_{a_j}$. By replacing "$a_j$" by "$b_k$" the operators $\hat{b}_k$ and $\hat{b}_k^+$ are defined for qubit b_k. In addition, we define the raising and lowering operators $\sigma = |g\rangle_{\rm c} \langle e|$ and $\sigma^+ = |e\rangle_{\rm c} \langle g|$ for the coupler C, which satisfy $[\sigma^+, \sigma] = \sigma_z$ with $\sigma_z = |e\rangle_{\rm c} \langle e| - |g\rangle_{\rm c} \langle g|$. The discussion below is based on Fig. 1(a). However, it should be mentioned that the results can directly apply to Fig. 1(b) to accomplish the same tasks, by mapping the large detuning conditions, required for the qubit pairs (a_1, b_1), (a_2, b_2),..., and (a_N, b_N), to the qubit pairs (a_1, b_2), (a_2, b_N),..., and (a_N, b_1) in Fig. 1(b), respectively.

In general, qubits a_j and b_k can be tuned to have the same detuning with respect to the coupler's transition frequency ω_C. However, for the sake of simplicity, we set $j = k$ in the following discussion. Suppose qubit a_j (b_j) is coupled to the coupler C, with coupling strength g_j (μ_j) and

detuning Δ_j. In the interaction picture, the Hamiltonian of the whole system is given by

$$H_I = \sum_{j=1}^{N} \left(g_j e^{i\Delta_j t} \hat{a}_j \sigma^+ + \mu_j e^{i\Delta_j t} \hat{b}_j \sigma^+ + \text{H.c.} \right), \tag{1}$$

where $\Delta_j = \omega_c - \omega_{aj} = \omega_c - \omega_{bj}$ (Fig. 2) and ω_{aj} (ω_{bj}) is the frequency of qubit a_j (b_j).

Under the large detuning condition $\Delta_j \gg g_j, \mu_j$, the two sets of qubits do not exchange energy with the coupler. However, the coupler can mediate N independent pair-wise superexchange interactions between the two sets of $2N$ qubits. Qubit a_j is only coupled to qubit b_j when the detunings satisfy the following conditions

$$\frac{|\Delta_j - \Delta_k|}{\Delta_j^{-1} + \Delta_k^{-1}} >> g_j g_k,\ g_j \mu_k,\ \mu_j \mu_k;\ j \neq k. \tag{2}$$

Then we obtain the effective Hamiltonian $H_{eff} = H_0 + H_{int}$, with

$$\begin{aligned} H_0 \ = \ & \sum_{j=1}^{N} \left(\frac{g_j^2}{\Delta_j} \hat{a}_j \hat{a}_j^\dagger + \frac{\mu_j^2}{\Delta_j} \hat{b}_j \hat{b}_j^\dagger \right) |e\rangle \langle e| \\ & - \sum_{j=1}^{N} \left(\frac{g_j^2}{\Delta_j} \hat{a}_j^\dagger \hat{a}_j + \frac{\mu_j^2}{\Delta_j} \hat{b}_j^\dagger \hat{b}_j \right) |g\rangle \langle g| , \end{aligned} \tag{3}$$

$$H_{int} = \sum_{j=1}^{N} \lambda_j (\hat{a}_j \hat{b}_j^\dagger + \hat{a}_j^\dagger \hat{b}_j)(|e\rangle \langle e| - |g\rangle \langle g|), \tag{4}$$

where $\lambda_j = g_j \mu_j / \Delta_j$. The first (second) term in the first bracket of H_0 is an ac-Stark shift of the level $|e\rangle$ of the coupler C, induced by the interaction with qubit a_j (b_j); while the first (second) term in the second bracket of H_0 is an ac-Stark shift of the level $|g\rangle$ of the two-level coupler, induced by the interaction with qubit a_j (b_j). Here and below, we have defined $|g\rangle \equiv |g\rangle_c$ and $|e\rangle \equiv |e\rangle_c$ for simplicity.

To simplify discussions hereafter we set $g_j = \mu_j$ and $\omega_{aj} = \omega_{bj} = \omega_j$ which can be realized readily by design and fabrication. Consequently, the qubits a_j and b_j have the same detuning Δ_j. It is also understood that $\omega_i \neq \omega_j$ and $g_i \neq g_j$ for $i \neq j$. In this way, each pair of qubits has its own unique frequency and qubit-coupler interaction strength while all pairs have the same effective coupler mediated interaction strength. In a new interaction picture with respect to the Hamiltonian H_0, we have $H'_{int} = e^{iH_0 t} H_{int} e^{-iH_0 t} = H_{int}$. When the coupler C is initially in the ground state $|g\rangle$, it will remain in this state throughout the interaction as the Hamiltonian H_{int} cannot induce any transition for the coupler. In this case, based on Eq. (4) and $H'_{int} = H_{int}$, the Hamiltonian H'_{int} is reduced to

$$H_e = -\sum_{j=1}^{N} \lambda_j (\hat{a}_j \hat{b}_j^\dagger + \hat{a}_j^\dagger \hat{b}_j), \tag{5}$$

which is the effective Hamiltonian governing the dynamics of the two sets of qubits.

The two sets of qubits can be any type of qubits such as bosonic qubits or atomic qubits (e.g., artificial atoms or natural atoms). In principle, we can employ this effective Hamiltonian to implement several fundamental quantum operations on two sets of qubits, such as entanglement swap, multi-qubit logic gates, and creation of quantum entanglement in or between two sets of qubits. As a concrete example, in the next section we explicitly show how to apply this Hamiltonian to implement TEAMS between two sets of bosonic qubits.

As a final note, we point out that the condition $g_j = \mu_j$ is unnecessary. As shown in the

Method, for the case of $g_j \neq \mu_j$, the effective Hamiltonian (5) can be obtained by setting the detuning of the qubit a_j slightly different from that of qubit b_j ($j = 1, 2, ..., N$).

Quantum state swapping and transfer. Let us go back to Fig. 1(a), where any initially unentangled state of the first set of N qubits $(a_1, a_2, ..., a_N)$ and the second set of N bosonic qubits $(b_1, b_2, ..., b_N)$ can be described by the joint state $|\psi_{\rm A}(0)\rangle \otimes |\psi_{\rm B}(0)\rangle$. Here, the first (second) part of the product is the initial state of the first (second) set of N qubits, taking a general form of $|\psi_{\rm A}(0)\rangle = \sum_{n_j=0}^{1} c_{\{n_j\}} \prod_{j=1}^{N} |n_j\rangle_{a_j}$ ($|\psi_{\rm B}(0)\rangle = \sum_{m_k=0}^{1} d_{\{m_k\}} \prod_{k=1}^{N} |m_k\rangle_{b_k}$). The subscript a_j (b_k) represents qubit a_j (b_k), $c_{\{n_j\}}$ is the coefficient of the component $\prod_{j=1}^{N} |n_j\rangle_{a_j}$ of the initial state for the qubits $(a_1, a_2, ..., a_N)$, and the same notation applies to $d_{\{m_k\}}$ for the qubits $(b_1, b_2, ..., b_N)$. In terms of $|1_j\rangle_{a_j} = \hat{a}_j^{\dagger} |0\rangle_{a_j}$ and $|1_k\rangle_{b_k} = \hat{b}_k^{\dagger} |0\rangle_{b_k}$, we can write down the initial state as

$$\begin{aligned} & |\psi_{\rm A}(0)\rangle \otimes |\psi_{\rm B}(0)\rangle \\ = & \sum_{n_j=0,1} c_{\{n_j\}} \sum_{m_k=0,1} d_{\{m_k\}} \prod_{j=1}^{N} \prod_{k=1}^{N} \left(\hat{a}_j^{+n_j} \hat{b}_k^{+m_k} |0\rangle_a |0\rangle_b \right), \end{aligned} \tag{6}$$

where $|0\rangle_a = |0\rangle_{a_1} ... |0\rangle_{a_N}$ and $|0\rangle_b = |0\rangle_{b_1} ... |0\rangle_{b_N}$.

For bosonic qubits, the operators $(\hat{a}_j, \hat{a}_j^{+})$ and $(\hat{b}_j, \hat{b}_j^{+})$ obey $\left[\hat{a}_j, \hat{a}_j^{+}\right] = \left[\hat{b}_j, \hat{b}_j^{+}\right] = 1$. The effective Hamiltonian H_e leads to the transformations $e^{-iH_e t} \hat{a}_j^{\dagger} e^{iH_e t} = \cos(\lambda_j t) \hat{a}_j^{\dagger} + i \sin(\lambda_j t) \hat{b}_j^{\dagger}$, and $e^{-iH_e t} \hat{b}_j^{\dagger} e^{iH_e t} = \cos(\lambda_j t) \hat{b}_j^{\dagger} + i \sin(\lambda_j) \hat{a}_j^{\dagger}$. These transformations have the following property: (i) by setting $|\lambda_j| = \lambda$, i.e., $g_j \mu_j / |\Delta_j| = \lambda$ (independent of j). This condition can be met by using frequency-tunable qubits (or resonators). In the case of fixed frequency resonators one can design and fabricate the qubits a_j and b_j to have the proper frequencies ($\omega_{aj} = \omega_{bj} = \omega_j$) and coupling strengths (g_j, μ_j) respectively and to set $|\Delta_j| = g_j \mu_j / \lambda$ accordingly, and (ii) for $\lambda t = \pi/2$, we

obtain $e^{-iH_e t}\hat{a}_j^{\dagger}e^{iH_e t}=i^{\lambda_j/\lambda}\hat{b}_j^{\dagger}$ and $e^{-iH_e t}\hat{b}_j^{\dagger}e^{iH_e t}=i^{\lambda_j/\lambda}\hat{a}_j^{\dagger}$. Accordingly, we have $e^{-iH_e t}\hat{a}_j e^{iH_e t}=-i^{\lambda_j/\lambda}\hat{b}_j$ and $e^{-iH_e t}\hat{b}_j e^{iH_e t}=-i^{\lambda_j/\lambda}\hat{a}_j$. These unitary transformations will be employed in the derivation of Eq. (7) below.

Under the Hamiltonian H_e, the state of the subsystem, consisting of the $2N$ qubits in sets A and B, after an evolution time $t=\pi/(2\lambda)$ is given by

$$\begin{aligned}
|\psi_{\mathrm{AB}}(t)\rangle &= e^{-iH_e t}\ |\psi_{\mathrm{A}}(0)\rangle\otimes|\psi_{\mathrm{B}}(0)\rangle \\
&= \sum_{n_j=0,1} c_{\{n_j\}} \sum_{m_k=0,1} d_{\{m_k\}} \prod_{j=1}^{N}\prod_{k=1}^{N} \\
&\quad \left[(i)^{n_j\lambda_j/\lambda}(i)^{m_k\lambda_k/\lambda}\left(\hat{b}_j^{\dagger}\right)^{n_j}\left(\hat{a}_k^{\dagger}\right)^{m_k}|0\rangle_a|0\rangle_b\right] \\
&= \sum_{m_k=0,1} d_{\{m_k\}} \prod_{k=1}^{N}(i)^{m_k\lambda_k/\lambda}|m_k\rangle_{a_k} \\
&\quad \otimes \sum_{n_j=0,1} c_{\{n_j\}} \prod_{j=1}^{N}(i)^{n_j\lambda_j/\lambda}|n_j\rangle_{b_j}\,, \qquad (7)
\end{aligned}$$

where $\lambda_j/\lambda=\pm1$ and $\lambda_k/\lambda=\pm1$. Note that in the last two lines of Eq. (7), the first part of the product represents the N-qubit state of $(a_1,a_2,...,a_N)$ while the second part is that of $(b_1,b_2,...,b_N)$.

After returning to the original interaction picture, the state of the whole system, $|\psi'_{\mathrm{ABC}}(t)\rangle = e^{-iH_0 t}|\psi_{\mathrm{AB}}(t)\rangle|\psi_{\mathrm{c}}(t)\rangle$, can be further written as $|\psi'_{\mathrm{ABC}}(t)\rangle=|\psi'_{\mathrm{AB}}(t)\rangle\otimes|g\rangle_{\mathrm{c}}$. By letting H_0 act on the state $|\psi_{\mathrm{AB}}(t)\rangle$, we obtain a decomposition of $|\psi'_{\mathrm{AB}}(t)\rangle=|\psi_{\mathrm{A}}(t)\rangle\otimes|\psi_{\mathrm{B}}(t)\rangle$ with

$$|\psi_{\mathrm{A}}(t)\rangle=\sum_{m_k=0,1} d_{\{m_k\}}\prod_{k=1}^{N}\left(e^{i\phi_k m_k\pi}|m_k\rangle_{a_k}\right), \qquad (8)$$

$$|\psi_{\mathrm{B}}(t)\rangle=\sum_{n_j=0,1} c_{\{n_j\}}\prod_{j=1}^{N}\left(e^{i\theta_j n_j\pi}|n_j\rangle_{b_j}\right), \qquad (9)$$

where $\phi_k = (\lambda_k + g_k^2/\Delta_k)/(2\lambda)$ and $\theta_j = (\lambda_j + \mu_j^2/\Delta_j)/(2\lambda)$. This is equivalent to the quantum state swap operation plus single-qubit phase shifts $e^{i\phi_k\pi}$ ($e^{i\beta_j\pi}$) on the state $|1\rangle$ of qubit a_k (b_j). These additional phase shifts can be corrected for by local single-qubit rotations $e^{-i\phi_k\pi\hat{a}_k^\dagger\hat{a}_k}$ and $e^{-i\theta_j\pi\hat{b}_j^\dagger\hat{b}_j}$. Notice that the multiplexed quantum state exchange protocol described above becomes the state transfer protocol by initializing all qubits in the second (i.e., receiving) set in the state $|0\rangle$. More importantly, because the states $|\psi_{\mathrm{A}}(0)\rangle$ and $|\psi_{\mathrm{B}}(0)\rangle$ considered above take a general form, the protocol can be applied directly to swap or transfer any type of multipartite entanglement, such as the GHZ state $|00...0\rangle + |11...1\rangle$, the W- state $\frac{1}{\sqrt{N}}(|00...001\rangle + |00...010\rangle + ... + |10...000\rangle)$, the cluster state, and so on, between the two sets of multiple qubits.

It should be mentioned that in reality a physical coupler usually has more than two levels. However, if the coupler is a nonlinear quantum element such as a superconducting qubit, population leakage out of the two-dimensional Hilbert space formed by $|g\rangle$ and $|e\rangle$ of the coupler can be made negligible by choosing proper coupler parameters. In contrast, when the coupler is a single-mode resonator [44], the probability of population leaking into higher energy levels of the coupler could be significant due to its uniform energy level spacing. This problem becomes apparent as the number of qubits increases.

Quantum dynamics of two bosonic qubits/resonators coupled by a superconducting qubit as a quantum switch has been studied previously in [45,46]. However, although our method of TEAMS is based on the same type of coupler mediated dispersive interaction between qubits described in [45,46] it is not a simple extension of the latter because that would require the use of

N couplers for N pairs of qubits/resonators. The distinctive feature of our method is to utilize the "frequency multiplexing" capability of our effective Hamiltonian to have each qubit in one set coupled uniquely to only one of the qubits in the other set and to have all N pair-wise interactions occur concurrently, so that one-step TEAMS between the two N-qubit sets with only one coupler qubit, rather than N couplers, becomes possible.

It is noted that if one chooses to perform TEAMS between two sets of resonators the preparation of the initial state of the resonators would in general require the use of qubits as well as tunable qubit-resonator couplings [47-50]. For example, this task could be accomplished by coupling one ancilla qubit to each resonator [51,52]. However, because the main objective of this work is to show how to perform TEAMS in a single step we assume the states to be transfered or exchanged already exist. Thus, we will not discuss the details of how to prepare the initial states of the resonators.

The TLC is assumed to be a frequency-tunable superconducting qubit (a.k.a. artificial atom) [53-56]. Generally speaking, it is highly desirable to use qubits with frequency and coupling strength (g_j and μ_j) both tunable to implement the proposed one-step TEAMS as the double tunability would provide great flexibility in satisfying all required conditions, in particular $|\lambda_j| = g_j\mu_j/|\Delta_j| = \lambda$. In practice, however, frequency tunability is readily available for artificial atoms and to a less extent for resonators [57,58] while tunable coupling strength is significantly more difficult to obtain.

We emphasize that assumption of uniform effective coupling strength is unnecessary and it

is only used for the convenience of discussion above. For instance, a manufactured circuit with fixed coupling strengths may have j-denpendent effective coupling strengths λ_j. In this case, the TEAMS cannot be completed by turning on/off the effective coupling for all pairs of qubits simultaneously. Fortunately, this problem can be circumvented by relaxing the strong condition to a weaker one: instead to require all λ_j's to have the same magnitude they can be different as long as the condition $\omega_{aj} = \omega_{bj} = \omega_j \neq \omega_{i\neq j}$ is still satisfied. The weaker condition can be met by using frequency tunable qubits or resonators. A simple case to consider is the qubit-coupler coupling strengths for all $2N$ qubits (resonators) are the same or approximately equal. Experimentally, this is the easiest to realize and most likely to be encountered. With this set up all one needs to do is to switch on the effective dispersive interaction between qubits a_j and b_j at a proper time $\tau_j = t_{\max} - t_j$ by tuning their frequencies to have the proper Δ_j, where $t_{\max} = \max(\pi/2\lambda_1, \pi/2\lambda_2, ... \pi/2\lambda_N)$ and $t_j = \pi/2\lambda_j$, and let it evolve for a time interval t_j before switching off the effective interaction λ_j. Consequently, at $t = t_{\max}$ all coupler mediated effective interactions are switched off which can be accomplished by tuning the $coupler$ frequency ω_c far way from that of all $2N$ qubits. In this last step the coupler is used essentially as a quantum switch [45,46] to simultaneously cut off the effective interaction between all pairs of qubits.

The coupling between the resonators and the coupler qubit can be effectively turned on (off) by adjusting the level spacings of the coupler qubit. When the coupler qubit frequency is highly detuned from the resonator frequencies the couplings are effectively switched off, and when the coupler qubit frequency is detuned from the resonator frequencies by a suitable amount they are dispersively coupled as the case discussed above. For a superconducting coupler qubit, the level

spacings can be readily adjusted by varying external control parameters (e.g., magnetic flux applied to phase, transmon, or flux qubits, see, e.g., [53-56]).

Experimental implementation. In practice, the proposed scheme can be implemented using either the artificial atoms (e.g., superconducting qubits) or resonators [e.g., superconducting coplanar waveguide (CPW) resonators] as the physical objects to demonstrate the proposed one-step TEAMS protocol. The artificial atoms have the advantage of tunnable frequency, better separation between the computational states from the non-computational ones because they are nonlinear oscillators, and the ease of initial state preparation. On the other hand, high-Q CPW resonator is comparatively easier to design and fabricate. For example, CPW resonators with quality factor on the order of 10^6 (i.e., about 30 μs of the lifetime of photons for a 6 GHz resonator) have been demonstrated with a single layer of sputtered superconducting films [59-61]. In addition, frequency tunnable resonators have also been demonstrated recently [57,58].

In the example discussed below, we choose resonators as the realization of bosonic qubits for the following reasons: (1) Systems of superconducting resonators and qubits have been considered one of the most promising candidates for quantum information processing [62-65] and there is a growing interest in quantum information processing based on microwave photon qubits. Within circuit QED, several theoretical proposals have been put forward for utilizing microwave photons stored in two superconducting CPW resonators as qubits/qudits for quantum gates [66-69]. (2) Microwave photons have been considered as candidates for quantum memories [58,70-72]. When performing quantum information processing, TEAMS between different multi-qubit mem-

ory banks would become a ubiquitous task. (3) Because it is in general more difficult to tune the frequency of the resonantors than artificial atoms and linear resonators are a poor realization of qubits, if our scheme can be demonstrated to work well with frequency and coupling strength non-tunable resonators it would work better and/or easier to implement with frequency tunable artificial atoms or resonators. Namely, we choose a more difficult case to study.

Let us now consider four fixed-frequency superconducting coplanar waveguide (CPW) resonators, capacitively coupled to a superconducting transmon coupler [73] as illustrated in Fig. 3. We emphasize again that using frequency tunable resonators would make the implementation considerably easier. For simplicity, we use (a_1, a_2, b_1, b_2) to denote the four qubits. For the setup here, a_j (b_j) is a bosonic mode of the resonator a_j (b_j), and the two logic states of the qubit a_j (b_j) are represented by the vacuum state and the single-photon state of the bosonic mode of resonators a_j (b_j) ($j = 1, 2$). In the following, we first present a general discussion on the fidelity of the operation. To quantify operation fidelity of the proposed protocol, we then numerically calculate the fidelity for transferring and exchanging each of the four Bell states $|\psi^{\pm}\rangle = \frac{1}{\sqrt{2}}(|01\rangle \pm |10\rangle)$ and $|\phi^{\pm}\rangle = \frac{1}{\sqrt{2}}(|00\rangle \pm |11\rangle)$ between the two pairs of qubits (i.e., the case of $N = 2$).

In the above discussions, we have considered each qubit as a two-level bosonic mode and defined the operators $\hat{a}_j, \hat{b}_j, \hat{a}_j^+$, and $\hat{b}_j^+$ using the two energy eigenstates $|0\rangle$ and $|1\rangle$ as the computational basis states. It is noted that during the operation, more than a single photon could reside in each resonator when the large detuning conditions (2) are not well satisfied. For this reason, we treat the above-defined operators $\hat{a}_j, \hat{b}_j, \hat{a}_j^+$,and $\hat{b}_j^+$ as the usual photon annihilation and creation

operators introduced in quantum optics. Note that after this replacement, the Hamiltonian H_I in the interaction picture, describing the interaction of the four resonators with the transmon coupler, takes the same form as that given in Eq. (1) with $N = 2$. By doing this, the effects of all excited states of the resonators are taken into account.

The numerical simulation is carried out by solving the master equation (10) which describes the dynamics of four resonators coupled to a superconducting transmon. As shown in Table I [59-61,74-77], the simulation takes the effects of dissipation and dephasing on the fidelity into account. Specifically, we selected a conservative set of resonator and transmon parameters in the numerical simulation to demonstrate experimental feasibility. In addition, assuming all coupling constants are equal $g_1 = \mu_1 = g_2 = \mu_2 \equiv g = 2\pi \times 100$ MHz (again this is an undesirable situation). The fidelity of the operations is given by $\mathcal{F} = \sqrt{\langle\psi_{id}|\,\widetilde{\rho}\,|\psi_{id}\rangle}$ [78], where $|\psi_{id}\rangle = |\psi_{\rm A}(t)\rangle\,|\psi_{\rm B}(t)\rangle\,|g\rangle_{\rm c}$, with $|\psi_{\rm A}(t)\rangle$ given in Eq. (8) and $|\psi_{\rm B}(t)\rangle$ in Eq. (9), is the output state for an ideal system (i.e., without dissipation, dephasing and leakage to high excited states) after completing the operations and $\widetilde{\rho}$ is the final density operator of the system.

The simulated fidelity as a function of the dimensionless detuning $\alpha \equiv \Delta/g$ in the range of $4 \leq \alpha \leq 10$ for Bell-state transfer and exchange are shown in Figs. 4 and 5, respectively. It is found that the maximum fidelity of transferring the four Bell states $|\psi^{\pm}\rangle$ and $|\phi^{\pm}\rangle$ from the resonators (a_1, a_2) to (b_1, b_2) or vice versa is equal to or better than 99.1%, when $\alpha \equiv \Delta/g = 5.5$. While for exchanging $|\psi^{+}\rangle$ with $|\psi^{-}\rangle$, $|\phi^{+}\rangle$ with $|\phi^{-}\rangle$, $|\phi^{\pm}\rangle$ with $|\psi^{+}\rangle$, and $|\phi^{\pm}\rangle$ with $|\psi^{-}\rangle$ the maximum fidelity is 97.2%, 96.3%, 96.4%, and 96.6%, respectively, obtained around $\alpha = 9.3$. Furthermore,

the high fidelity is hardly affected by weak residual inter-resonator crosstalks as often the case in experimental situations (see Supplementary Information). However, it should be pointed out that the value of the detuning parameter α at which the maximum fidelity is achieved depends on other parameters, such as the photon decay rate, of the resonators and thus is not universal. In experiments, α needs to be fine tuned to obtain the maximum fidelity.

As discussed previously, one of the advantages of the single-step TEAMS method proposed here is that the coupler remains separable from the qubits and it stays mostly in the ground state so that the effects of coupler's decoherence on the fidelity of TEAMS is significantly reduced. To confirm this property numerical simulations were performed and the result confirms that for Bell-state transfer (exchange) the time-averaged population of the coupler's excited state $|e\rangle$ is $0.03 \leq \overline{P}_e \leq 0.08$ ($0.03 \leq \overline{P}_e \leq 0.05$) for the operations described above.

As the above example and parameters listed in Table 1 show, our scheme does not require the use of tunable resonator-coupler coupling strength and/or tunable frequency resonators. Furthermore, $g_j = \mu_j$ is not a necessary condition and it is chosen only to simplify discussions. The strong condition that needs to be satisfied for simultaneous TEAMS is the effective pair-wise coupling strength $\lambda_j = g_j\mu_j/\Delta_j$ should have the same value for all $j = 1, 2, ..N$ qubit pairs. Therefore, our scheme does not require, though it would be more convenient, to have tunable resonator-qubit coupling strength g_j and μ_j. For example, it is straightforward to design and to fabricate pairs of resonators a_j and b_j to have j-dependent frequency ω_j and coupling strength g_j such that $|\lambda_j| = g_j^2/|\Delta_j| = \lambda$.

The advantage of utilizing positive as well as negative detunings is worth to discuss. Because our scheme essentially explores the frequency multiplexing property of the effective Hamiltonian (5) it will encounter the "frequency crowding" problem. Because the system dynamics does not depend on the signs of detunings according to Eqs. (6-8), utilizing the positive as well as the negative detunings would double the maximum number of qubits that can be accommodated by a given circuit. This advantage is most clearly demonstrated by the example presented above: when all four resonators have the same couplig strength to the coupler the only way to satisfy $\lambda_1 = |\lambda_2| = \lambda$ is to have $\Delta_1 = -\Delta_2$.

We would like to point out that although the proposed scheme of TEAMS can be implemented using a small number of qubits or resonators with fixed frequency and/or coupling strength it is in general diserable and even necessary to have the frequency tunability for a moderate number of qubits or resonators. This is especially true if one wants to realize the reconfigurable network as that of illustrated in Fig. 1. Note that tunable frequency artificial atoms are readily available and tunable superconducting resonators have been demonstrated by incorporating nonlinear elements, such as a small dc SQUID, into the design [57,58].

Discussion

We have shown that the minimum hardware resources required for simultaneously transferring or swapping arbitrary multipartite quantum states between two sets of otherwise noninteracting qubits each having a 2^N-dimensional Hilbert space can be achieved using a single two-level coupler. This

result means that arbitrary N-qubit states that span a 2^N-dimensional Hilbert space can be transferred or exchanged between two N-qubit registers in a single step via a coupler whose Hilbert space is 2-dimensional only. In addition, during the entire process the coupler remains separable from the qubits and stays mostly in the ground state throughout the entire process thus suppressing the undesirable effects of coupler decoherence. The finding of the minimum resource required and the method to simultaneously transfer or swap arbitrary N-partite states in a single step is of great interest and fundamental importance in quantum information science. If realized experimentally, it would be a big step forward in the direction of building scalable quantum information processing networks because in principle the operation time required is independent of the number of qubits involved. In addition, as a concrete example we show that transferring (exchanging) the Bell states between two pairs of resonators (bosonic qubits) interacting via a superconducting transmon coupler can achieve fidelity as high as 99.1% (no less than 96.3%) with conservative device and circuit parameters. In addition, because the method does not use classical pulses during the entire operation and the constituents of the two registers can be reassigned *in situ* through the reconfigurable coupler-mediated pair interaction described by Eq. (4) and illustrated in Fig. 1(b), the proposed scheme can greatly reduce the complexity of the circuit and can serve as one of the fundamental building block for the development of more sophisticated quantum network architectures in the future. Finally, the result presented here is general and thus in principle can be applied to any type of physical qubits such as electronic and nuclear spins, photons, atoms, and artificial atoms.

Methods

Master equation. When the dissipation and dephasing are included, the dynamics of the open system is determined by the following master equation

$$\begin{aligned}\frac{d\rho}{dt} &= -i\left[H_I,\rho\right]+\sum_{j=1}^{2}\kappa_{a_j}\mathcal{L}\left[\hat{a}_j\right]+\sum_{j=1}^{2}\kappa_{b_j}\mathcal{L}\left[\hat{b}_j\right] \\ &\quad +\gamma\mathcal{L}\left[\sigma\right]+\gamma_{\varphi}\left(\sigma_z\rho\sigma_z-\rho\right), \end{aligned} \tag{10}$$

where H_I is the interaction Hamiltonian given in Eq. (1), $\sigma_z = |e\rangle\langle e| - |g\rangle\langle g|$, and $\mathcal{L}[\Lambda] = \Lambda\rho\Lambda^{+} - \Lambda^{+}\Lambda\rho/2 - \rho\Lambda^{+}\Lambda/2$ (with $\Lambda = \hat{a}_j, \hat{b}_j, \sigma$). In addition, κ_{a_j} (κ_{b_j}) is the decay rate of the resonator mode a_j (b_j); γ is the energy relaxation rate for the level $|e\rangle$; and γ_{φ} is the dephasing rate of the level $|e\rangle$ of the coupler**.**

Effective Hamiltonian for non-identical coupling strengths and detunings. Suppose that qubit a_j (b_j) is coupled to the coupler C, with coupling strength g_j (μ_j) and detuning Δ_{a_j} (Δ_{b_j}). In the interaction picture, the Hamiltonian of the whole system is given by

$$H_I = \sum_{j=1}^{N}\left(g_j e^{i\Delta_{a_j}t}\hat{a}_j\sigma^{+} + \mu_j e^{i\Delta_{b_j}t}\hat{b}_j\sigma^{+} + \text{H.c.}\right), \tag{11}$$

where $\Delta_{a_j} = \omega_{\text{c}} - \omega_{a_j}$ and $\Delta_{b_j} = \omega_{\text{c}} - \omega_{b_j}$.

Under the large detuning condition $\Delta_{a_j} \gg g_j$ and $\Delta_{b_j} \gg \mu_j$, and when the detunings satisfy the following condition

$$\frac{\left|\Delta_{\alpha_j} - \Delta_{\beta_k}\right|}{\Delta_{\alpha_j}^{-1} + \Delta_{\beta_k}^{-1}} \gg g_j g_k, \mu_j\mu_k, g_j\mu_k; j \neq k \tag{12}$$

(where $\alpha_j \in \{a_j, b_j\}$ and $\beta_k \in \{a_k, b_k\}$), we can obtain the effective Hamiltonian $H_{eff} = H_0 +$

H_{int}, with

$$\begin{aligned} H_0 &= \sum_{j=1}^{N}\left(\frac{g_j^2}{\Delta_{a_j}}\hat{a}_j\hat{a}_j^\dagger+\frac{\mu_j^2}{\Delta_{b_j}}\hat{b}_j\hat{b}_j^\dagger\right)|e\rangle\langle e| \\ &\quad -\sum_{j=1}^{N}\left(\frac{g_j^2}{\Delta_{a_j}}\hat{a}_j^\dagger\hat{a}_j+\frac{\mu_j^2}{\Delta_{b_j}}\hat{b}_j^\dagger\hat{b}_j\right)|g\rangle\langle g|, \end{aligned} \tag{13}$$

$$H_{int}=\sum_{j=1}^{N}\lambda_j\left[e^{i(\Delta_{a_j}-\Delta_{b_j})t}\hat{a}_j\hat{b}_j^\dagger+\text{H.c.}\right](|e\rangle\langle e|-|g\rangle\langle g|), \tag{14}$$

where $\lambda_j=\frac{g_j\mu_j}{2}(\Delta_{a_j}^{-1}+\Delta_{b_j}^{-1})$. When the coupler C is initially in the ground state $|g\rangle$, it will remain in this state as the Hamiltonians H_0 and H_{int} cannot induce any transition for the coupler. In this case, the Hamiltonians H_0 and H_{int} reduce to

$$H_0=-\sum_{j=1}^{N}\left(\frac{g_j^2}{\Delta_{a_j}}\hat{a}_j^\dagger\hat{a}_j+\frac{\mu_j^2}{\Delta_{b_j}}\hat{b}_j^\dagger\hat{b}_j\right)|g\rangle\langle g|, \tag{15}$$

$$H_{int}=-\sum_{j=1}^{N}\lambda_j\left[e^{i(\Delta_{a_j}-\Delta_{b_j})t}\hat{a}_j\hat{b}_j^\dagger+\text{H.c.}\right]|g\rangle\langle g|, \tag{16}$$

In a new interaction picture with respect to the Hamiltonian H_0, we obtain

$$\begin{aligned} H'_{int} &= e^{iH_0t}H_{int}e^{-iH_0t} \\ &= -\sum_{j=1}^{N}\lambda_j\left[e^{i(g_j^2/\Delta_{a_j}-\mu_j^2/\Delta_{b_j})t}e^{i(\Delta_{a_j}-\Delta_{b_j})t}\hat{a}_j\hat{b}_j^\dagger+\text{H.c.}\right]|g\rangle\langle g|. \end{aligned} \tag{17}$$

For the setting

$$g_j^2/\Delta_{a_j}-\mu_j^2/\Delta_{b_j}=-(\Delta_{a_j}-\Delta_{b_j}), \tag{18}$$

the Hamiltonian (17) becomes

$$H'_{int}=-\sum_{j=1}^{N}\lambda_j(\hat{a}_j\hat{b}_j^\dagger+\hat{a}_j^\dagger\hat{b}_j)|g\rangle\langle g|, \tag{19}$$

which is exactly the one given in Eq. (5) after dropping the atomic operator $|g\rangle\langle g|$.

Note that condition (18) can be achieved by setting

$$\Delta_{b_j} = \frac{\Delta_{a_j}^2 + g_j^2 + \sqrt{(\Delta_{a_j}^2 + g_j^2)^2 - 4\Delta_{a_j}^2\mu_j^2}}{2\Delta_{a_j}}. \tag{20}$$

For $g_j = \mu_j$, we have $\Delta_{b_j} = \Delta_{a_j}$, i.e., the case that we discussed previously. In constrast, for $g_j \neq \mu_j$, we have $\Delta_{b_j} \neq \Delta_{a_j}$ from Eq. (20). This result implies that if the coupling g_j is not equalivent to μ_j, one can still obtain the *time-independent* effective Hamiltonian (5) or (19) by setting the detuning Δ_{b_j} slightly different from Δ_{a_j}.

1. P. W. Shor, in Proceedings of the 35th Annual Symposium on Foundations of Computer Science, edited by S. Goldwasser (IEEE Computer Society Press, Los Alamitos, CA, 1994), Vol. 124.

2. Ekert, A. K., Quantum cryptography based on Bell's theorem. *Phys. Rev. Lett.* **67**(6), 661-663 (1991).

3. Bennett, C. H., Brassard G. & Mermin N. D. Quantum cryptography without Bell¡s theorem. *Phys. Rev. Lett.* **68**(5), 557-559 (1992).

4. Cirac, J. I. & Zoller, P. Quantum Computations with Cold Trapped Ions. *Phys. Rev. Lett.* **74**, 4091-4094 (1995).

5. Loss, D. & Divincenzo, D. P. Quantum computation with quantum dots. *Phys. Rev. A* **57**, 120-126 (1998).

6. Bennett, C. H. Quantum cryptography using any two nonorthogonal states. *Phys. Rev. Lett.* **68**, 3121-3124 (1992).

7. Bennett, C. H. *et al.* Teleporting an unknown quantum state via dual classical and Einstein-Podolsky-Rosen channels. *Phys. Rev. Lett.* **70**, 1895-1899 (1993).

8. Moussa, M. H. Y. Teleportation with identity interchange of quantum states. *Phys. Rev. A* **55**, R3287-3290 (1997).

9. Nielsen, M. A. & Caves, C. M. Reversible quantum operations and their application to teleportation. *Phys. Rev. A* **55**, 2547-2556 (1997).

10. Bužek, V. & Hillery, M. Quantum copying: Beyond the no-cloning theorem. *Phys. Rev. A* **54**, 1844-1852 (1996).

11. Bužek, V. , Braunstein, S. L., Hillery, M. & Bruß, D. Quantum copying: A network. *Phys. Rev. A* **56**, 3446-3452 (1997).

12. Yu, T. & Eberly, J. H. Sudden Death of Entanglement. *Science* **323**, 598-601 (2009).

13. Huang, Y. F. *et al.* Experimental generation of an eight-photon GreenbergerCHorneCZeilinger state. *Nat. Commun.* **2**, 546 (2011).

14. Yao, X. C. *et al.* Observation of eight-photon entanglemen. *Nat. Photonics* **6**, 225-228 (2012).

15. Monz, T. *et al.* 14-Qubit Entanglement: Creation and Coherence. *Phys. Rev. Lett.* **106**, 130506 (2011).

16. Hagley, E. *et al.* Generation of Einstein-Podolsky-Rosen Pairs of Atoms. *Phys. Rev. Lett.* **79**, 1-5 (1997).

17. Osnaghi, S. *et al.* Coherent Control of an Atomic Collision in a Cavity. Phys. Rev. Lett. **87**, 037902 (2001).

18. Chen, G. *et al.* Optically Induced Entanglement of Excitons in a Single Quantum Dot. *Science* **289**, 1906-1909 (2000).

19. Dolde, F. *et al.* High-fidelity spin entanglement using optimal control. *Nat. Commun.* **5**, 3371 (2013).

20. Leek, P. J. *et al.* Using sideband transitions for two-qubit operations in superconducting circuits. *Phys. Rev. B* **79**, 180511(R) (2009).

21. DiCarlo, L. *et al.* Demonstration of two-qubit algorithms with a superconducting quantum processor. *Nature* **460**, 240-244 (2009).

22. Ansmann, M. *et al.* Violation of Bell's inequality in Josephson phase qubits. *Nature* **461**, 504-506 (2009).

23. Chow, J. M. *et al.* Detecting highly entangled states with a joint qubit readout. *Phys. Rev. A* **81**, 062325 (2010).

24. DiCarlo, L. *et al.* Preparation and measurement of three-qubit entanglement in a superconducting circuit. *Nature* **467**, 574-578 (2010).

25. Barends, R. *et al.* Superconducting quantum circuits at the surface code threshold for fault tolerance. *Nature* **508**, 500-503 (2014).

26. Galvão, E. F. & Hardy, L. Building multiparticle states with teleportation. *Phys. Rev. A* **62**, 012309 (2000).

27. Johnson, T. J., Bartlett, S. D. & Sanders, B. C. Continuous-variable quantum teleportation of entanglement. *Phys. Rev. A* **66**, 042326 (2002).

28. Bowen, W. P. *et al.* Experimental investigation of continuous-variable quantum teleportation. *Phys. Rev. A* **67**, 032302 (2003).

29. Gordon, G. & Rigolin, G. Generalized teleportation protocol. *Phys. Rev. A* **73**, 042309 (2006).

30. Taketani, B. G., de Melo, F. & de Matos Filho, R. L. Optimal teleportation with a noisy source. *Phys. Rev. A* **85**, 020301(R) (2012).

31. Bouwmeester, D.*et al.* Experimental quantum teleportation. *Nature* **390**, 575-579 (1997).

32. Furusawa, A. *et al.* Unconditional Quantum Teleportation. *Science* **282**, 706-709 (1998).

33. Lee, N., Benichi, H., Takeno, Y., Takeda, S., Webb, J., Huntington, E. & Furusawa, A. Teleportation of Nonclassical Wave Packets of Light. *Science* **332**, 330-333 (2011).

34. Jin, X. M. *et al.* Experimental free-space quantum teleportation. *Nature Photonics* **87**, 376-381 (2010).

35. Yin, J. *et al.* Quantum teleportation and entanglement distribution over 100-kilometre free-space channels. Nature **488**, 185-188 (2012).

36. Baur, M., Fedorov, A., Steffen, L., Filipp, S., da Silva, M. P. & Wallraff, A. Benchmarking a Quantum Teleportation Protocol in Superconducting Circuits Using Tomography and an Entanglement Witness. *Phys. Rev. Lett.* **108**, 040502 (2012).

37. Steffen, L. *et al.* Deterministic quantum teleportation with feed-forward in a solid state system. *Nature* **500**, 319-322 (2013).

38. Majer, J. *et al.* Coupling superconducting qubits via a cavity bus. *Nature* **449**, 443-447 (2007).

39. Sillanpää, M. A., Park, J. I. & Simmonds, R. W. Coherent quantum state storage and transfer between two phase qubits via a resonant cavity. *Nature* **449**, 438-442 (2007).

40. Cirac, J. I., Zoller, P., Kimble, H. J. & Mabuchi, H. Quantum State Transfer and Entanglement Distribution among Distant Nodes in a Quantum Network. *Phys. Rev. Lett.* **78**, 3221-3224 (1997).

41. Pellizzari, T. Quantum Networking with Optical Fibres. *Phys. Rev. Lett.* **79**, 5242-5245 (1997).

42. Serafini, A., Mancini, S. & Bose, S. Distributed Quantum Computation via Optical Fibers. *Phys. Rev. Lett.* **96**, 010503 (2006).

43. Ritter, S. *et al.* An elementary quantum network of single atoms in optical cavities. *Nature* **484**, 195-200 (2012).

44. Zheng, S. B. & Guo, G. C. Efficient Scheme for Two-Atom Entanglement and Quantum Information Processing in Cavity QED. *Phys. Rev. Lett.* **85**, 2392-2395 (2000).

45. Mariantoni, M., Deppe, F., Marx, A., Gross, R., Wilhelm, F. K. & Solano, E. Two-resonator circuit quantum electrodynamics: A superconducting quantum switch. *Phys. Rev. Lett.* **78**, 104508 (2008).

46. Reuther, G. M. *et al.* Two-resonator circuit quantum electrodynamics: Dissipative theory. *Phys. Rev. B* **81**, 144510 (2010).

47. Niskanen, A. O. *et al.* Quantum coherent tunable coupling of superconducting qubits. *Science* **316**, 723-726 (2007).

48. Allman, M. S. *et al.* rf-SQUID-Mediated Coherent Tunable Coupling between a Superconducting Phase Qubit and a Lumped-Element Resonator. *Phys. Rev. Lett.* **104**, 177004 (2010).

49. Bialczak, R. C. *et al.* Fast Tunable Coupler for Superconducting Qubits. *Phys. Rev. Lett.* **106**, 060501 (2011).

50. Gambetta, J. M., Houck, A. A. & Blais A. Superconducting Qubit with Purcell Protection and Tunable Coupling. *Phys. Rev. Lett.* **106**, 030502 (2011).

51. Hofheinz, M. *et al.* Synthesizing arbitrary quantum states in a superconducting resonator. *Nature* **459**, 546-549 (2009).

52. Wang, H. *et al.* Deterministic entanglement of photons in two superconducting microwave resonators. *Phys. Rev. Lett.* **106**, 060401 (2011).

53. Clarke, J. & Wilhelm, F. K. Superconducting quantum bits. *Nature* **453**, 1031-1042 (2008).

54. Neeley, M. *et al.* Process tomography of quantum memory in a Josephson-phase qubit coupled to a two-level state. *Nature Phys.* **4**, 523-526 (2008).

55. Leek, P. J. *et al.* Using sideband transitions for two-qubit operations in superconducting circuits. *Phys. Rev. B* **79**, 180511(R) (2009).

56. Strand, J. D. *et al.* First-order sideband transitions with flux-driven asymmetric transmon qubits. *Phys. Rev. B* **87**, 220505(R) (2013).

57. Sandberg, M. *et al.* Tuning the field in a microwave resonator faster than the photon lifetime. *Appl. Phys. Lett.* **92**, 203501 (2008).

58. Wang, Z. L., Zhong, Y. P., He, L. J, Wang, H., Martinis, J. M., Cleland, A. N. & Xie, Q. W. Quantum state characterization of a fast tunable superconducting resonator. *Appl. Phys. Lett.* **102**, 163503 (2013).

59. Chen, W., Bennett, D. A., Patel, V. & Lukens, J. E. Substrate and process dependent losses in superconducting thin film resonators. *Supercond. Sci. Technol.* **21**, 075013 (2008).

60. Leek, P. J. *et al.* Cavity Quantum Electrodynamics with Separate Photon Storage and Qubit Readout Modes. *Phys. Rev. Lett.* **104**, 100504 (2010).

61. Megrant, A. *et al.* Planar superconducting resonators with internal quality factors above one million. *Appl. Phys. Lett.* **100**, 113510 (2012).

62. Blais, A., Huang, R. S., Wallraff, A., Girvin, S. M. & Schoelkopf, R. J. Cavity quantum electrodynamics for superconducting electrical circuits: An architecture for quantum computation. *Phys. Rev. A* **69**, 062320 (2004).

63. You, J. Q. & Nori, F. Atomic physics and quantum optics using superconducting circuits. *Nature* **474**, 589-597 (2011).

64. Xiang, Z. L., Ashhab, S., You, J. Q. & Nori, F. Hybrid quantum circuits: Superconducting circuits interacting with other quantum systems. *Rev. Mod. Phys.* **85**, 623-653 (2013).

65. Yang, C. P., Chu, S. I. & Han, S. Possible realization of entanglement, logical gates, and quantum-information transfer with superconducting-quantum-interference-device qubits in cavity QED. *Phys. Rev. A* **67**, 042311 (2003).

66. Schuster, D. I. *et al*. Resolving photon number states in a superconducting circuit. *Nature* **445**, 515-518 (2007).

67. Strauch, F. W. Quantum logic gates for superconducting resonator qudits. *Phys. Rev. A* **84**, 052313 (2011).

68. Wu, C. W, Gao, M., Li, H. Y., Deng, Z. J., Dai, H. Y., Chen, P. X. & Li, C. Z. Scalable one-way quantum computer using on-chip resonator qubits. *Phys. Rev. A* **85**, 042301 (2012).

69. Hua, M., Tao, M. J. & Deng, F. G. Universal quantum gates on microwave photons assisted by circuit quantum electrodynamics. *Phys. Rev. A* **90**, 012328 (2014).

70. Lucero, E. *et al.* Computing prime factors with a Josephson phase qubit quantum processor. *Nature Phys.* **8**, 719-723 (2012).

71. Pierre, M., Svensson, I. M., Sathyamoorthy, S. R., Johansson, G. & Delsing, P. Storage and on-demand release of microwaves using superconducting resonators with tunable coupling. *Appl. Phys. Lett.* **104**, 232604 (2014).

72. Mariantoni, M. *et al.* Implementing the quantum von neumann architecture with superconducting circuits. *Science* **334**, 61-65 (2011).

73. Koch, J. *et al.* Charge-insensitive qubit design derived from the Cooper pair box. *Phys. Rev. A* **76**, 042319 (2007).

74. Chang, J. B. *et al.* Improved superconducting qubit coherence using titanium nitride. *Appl. Phys. Lett.* **103**, 012602 (2013).

75. Paik, H. *et al.* Observation of High Coherence in Josephson Junction Qubits Measured in a Three-Dimensional Circuit QED Architecture. *Phys. Rev. Lett.* **107**, 240501 (2011).

76. Chow, J. M. *et al.* Implementing a strand of a scalable fault-tolerant quantum computing fabric. *Nat. Commun.* **5**, 4015 (2014).

77. Fedorov, A., Steffen, L., Baur, M., da Silva, M. P. & Wallraff, A. Implementation of a Toffoli gate with superconducting circuits. *Nature* **481**, 170-172 (2012).

78. Nielsen, M. A. & Chuang I. L. Quantum Computation and Quantum Information (Cambridge University Press, Cambridge, England, 2001).

Acknowledgments S. Han acknowledges support from NSF of the United States (PHY-1314861) and partial support by DMEA. S.B. Zheng was supported by the Major State Basic Research Development Program of China under Grant No. 2012CB921601. Q.P.S. was supported by the National Natural Science Foundation of China under Grant No. 11247008. C.P.Y. was supported in part by the National Natural Science Foundation of China under Grant Nos. 11074062 and 11374083, the Zhejiang Natural Science Foundation under Grant No. LZ13A040002, and the funds from Hangzhou Normal University under Grant Nos. HSQK0081 and PD13002004. This work was also supported by the funds from Hangzhou City for the Hangzhou-City Quantum Information and Quantum Optics Innovation Research Team.

Author contributions C.P.Y., S.B.Z. and S.H. carried out analytical calculations and wrote the main manuscript text. Q.P.S. performed numerical simulation. All authors participated in discussing the results and contributed to the interpretation of the work.

Additional information Competing financial interests: The authors declare no competing financial interests.

Table 1: Parameters for a transmon-coupled multi-resonator system. The values of ω_{a_j}, ω_{b_j}, Q_{a_j}, and Q_{b_j} ($j = 1, 2$) are estimated for $\alpha = 5.5$ (Bell-state transfer), $\alpha = 9.3$ (Bell-state exchange), $\omega_c/2\pi = 6.5$ GHz, and $g/2\pi = 100$ MHz. Here, $Q_{a_j} = \omega_{a_j}\kappa_{a_j}^{-1}$ and $Q_{b_j} = \omega_{b_j}\kappa_{b_j}^{-1}$. T_1 and T_2 can be made to be on the order of $20 - 60$ μs for state-of-the-art superconducting transom devices [74-76]. Superconducting CPW (coplanar waveguide) resonators with a quality factor $Q \sim 10^6$ have been experimentally demonstrated [59-61]. In addition, the coupling strength $g/2\pi \sim 360$ MHz has been reported for a superconducting transmon qubit coupled to a one-dimensional standing-wave CPW resonator [77].

Figure 1: Two sets of qubits coupled by a two-level coupler C. Here, the large circle at the center represents the two-level coupler C, the smaller circles on the left (right) indicate the N qubits $a_1, a_2, ..., a_N$ ($b_1, b_2, ..., b_N$) in the register A (B) connected to the coupler C by lines with the same color form an interacting qubit pair. In (a), the N pairs of qubits are (a_1, b_1), (a_2, b_2),..., and (a_N, b_N); while in (b) the N pairs of qubits are randomly chosen as, e.g., (a_1, b_2), (a_2, b_N),..., and (a_N, b_1). For (a) and (b), arbitrary N-partite states can be transferred or exchanged between A and B. In addition, various entangled states of qubits in A and B can be generated by the same coupler mediated qubit-qubit interaction.

Figure 2: Illustration of qubit-coupler dispersive interaction. The two horizontal solid lines represent the two energy levels of the coupler C. The bottom dashed line represents the common ground energy level of the $2N$ qubits, while the top dashed lines in different colors represent the higher energy levels of the $2N$ qubits, respectively. A vertical line, linked to the bottom dashed

line and a top dashed line, represents the level spacing between the two energy levels of a qubit. The frequency of qubit a_j (b_j) is labelled as ω_{aj} (ω_{bj}) (not shown), while the frequency of the coupler C is denoted as ω_c (not shown). Qubit a_j (b_j) is dispersively coupled to the coupler C with coupling constant g_j (μ_j) and detuning Δ_j ($j = 1, 2, ..., N$). Here, $\Delta_j = \omega_{\rm c} - \omega_{aj} = \omega_{\rm c} - \omega_{bj}$.

Figure 3: Setup for four resonators a_1, a_2, b_1, b_2 coupled by a superconducting transmon coupler (i.e., the circle C). Each resonator here is a one-dimensional coplanar waveguide resonator. The superconducting transmon qubit is capacitively coupled to each resonator via a capacitance.

Figure 4: Fidelity versus α for the Bell-state transfer. Here, the red and blue curves correspond to transferring the two Bell states $|\psi^+\rangle$ and $|\psi^-\rangle$, respectively. Numerical simulation shows that the fidelity for transferring the other two Bell states $|\phi^\pm\rangle$ is the same (the green line).

Figure 5: Fidelity versus α for the Bell-state exchange. Here, the red, blue, green, and yellow curves correspond to exchanging the Bell states, $|\psi^+\rangle$ with $|\psi^-\rangle$, $|\phi^+\rangle$ with $|\phi^-\rangle$, $|\phi^\pm\rangle$ with $|\psi^+\rangle$, and $|\phi^\pm\rangle$ with $|\psi^-\rangle$, between the qubit pairs (a_1, a_2) and (b_1, b_2), respectively.

[tbp] Table 1

Parameter	Symbol	Bell-state exchange	Bell-state transfer
Resonator photon lifetime	$\kappa_{a_1}^{-1}, \kappa_{b_1}^{-1}, \kappa_{a_2}^{-1}, \kappa_{b_2}^{-1}$	$1\ \mu$s	$1\ \mu$s
Coupler energy relaxation time	γ^{-1}	$3\ \mu$s	$3\ \mu$s
Coupler dephasing time	γ_{φ}^{-1}	$3\ \mu$s	$3\ \mu$s
Coupler frequency	$\omega_c/2\pi$	6.0 GHz	6.0 GHz
Resonator frequency, pair I	$\omega_{a_1}/2\pi, \omega_{b_1}/2\pi$	5.07 GHz	5.45 GHz
Resonator frequency, pair II	$\omega_{a_2}/2\pi, \omega_{b_2}/2\pi$	6.93 GHz	6.55 GHz
Resonator quality factor, pair I	Q_{a_1}, Q_{b_1}	3.2×10^4	3.4×10^4
Resonator quality factor, pair II	Q_{a_2}, Q_{b_2}	4.4×10^4	4.1×10^4

Figure 1

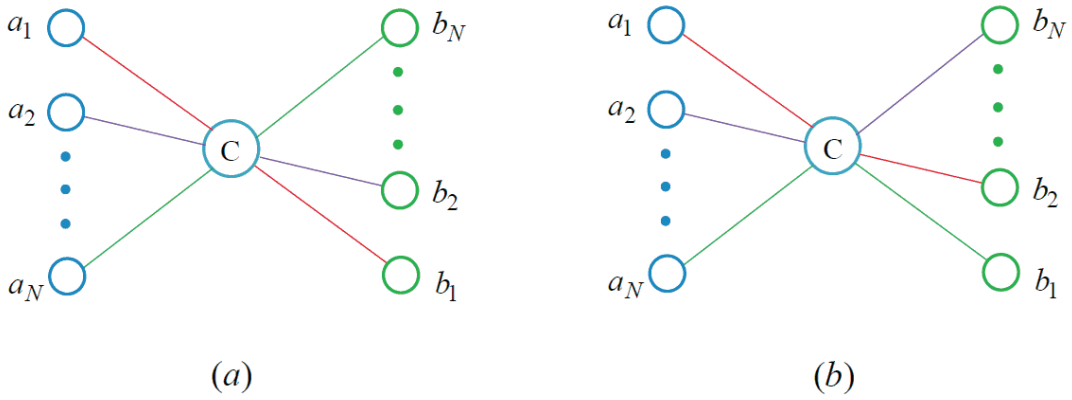

Figure 2

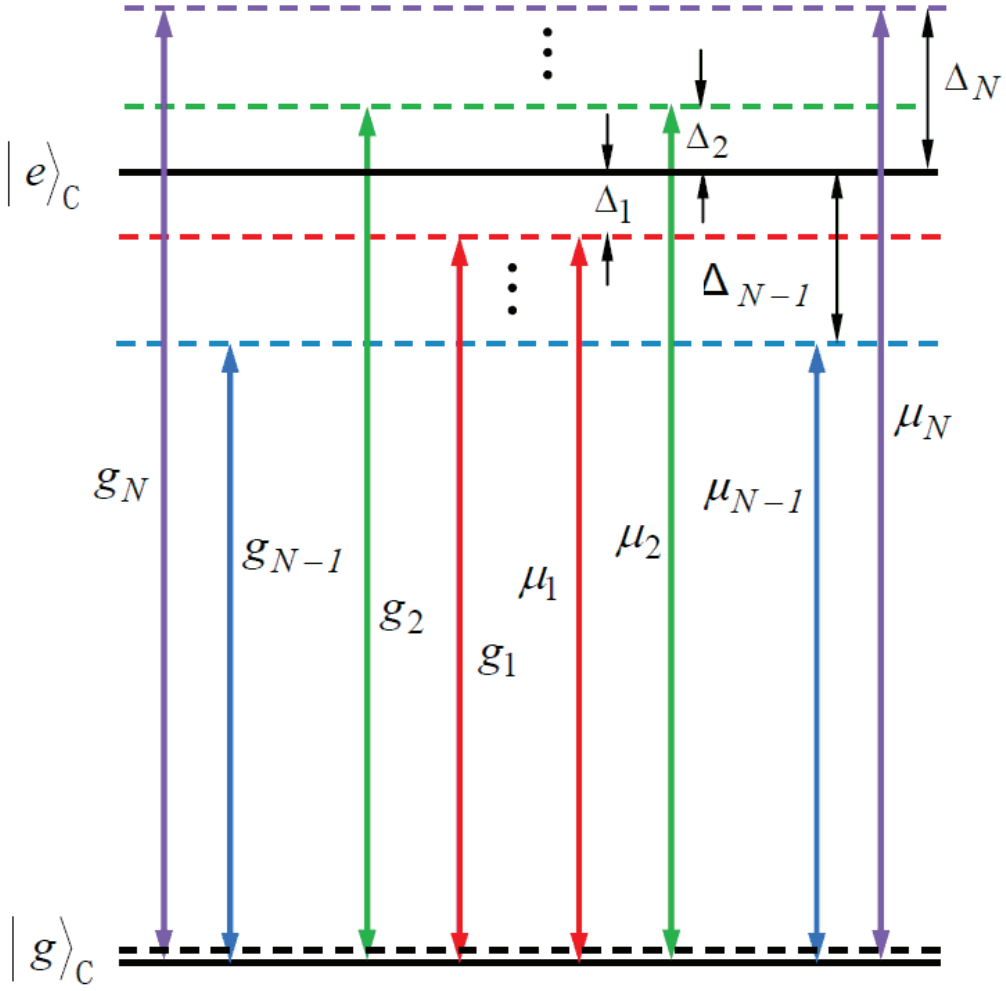
Δ_N
Δ_2
Δ_1
Δ_{N-1}
$|e\rangle_C$
$|g\rangle_C$
g_N
g_{N-1}
g_2
g_1
μ_1
μ_2
μ_{N-1}
μ_N

Figure 3

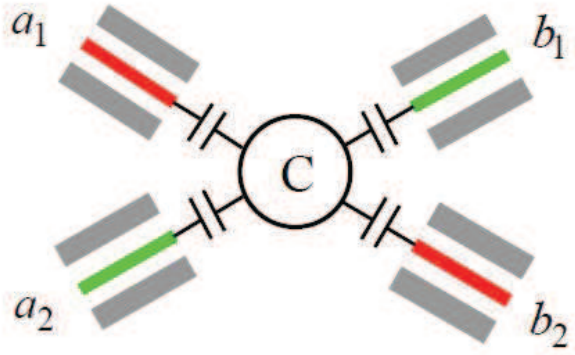

Figure 4

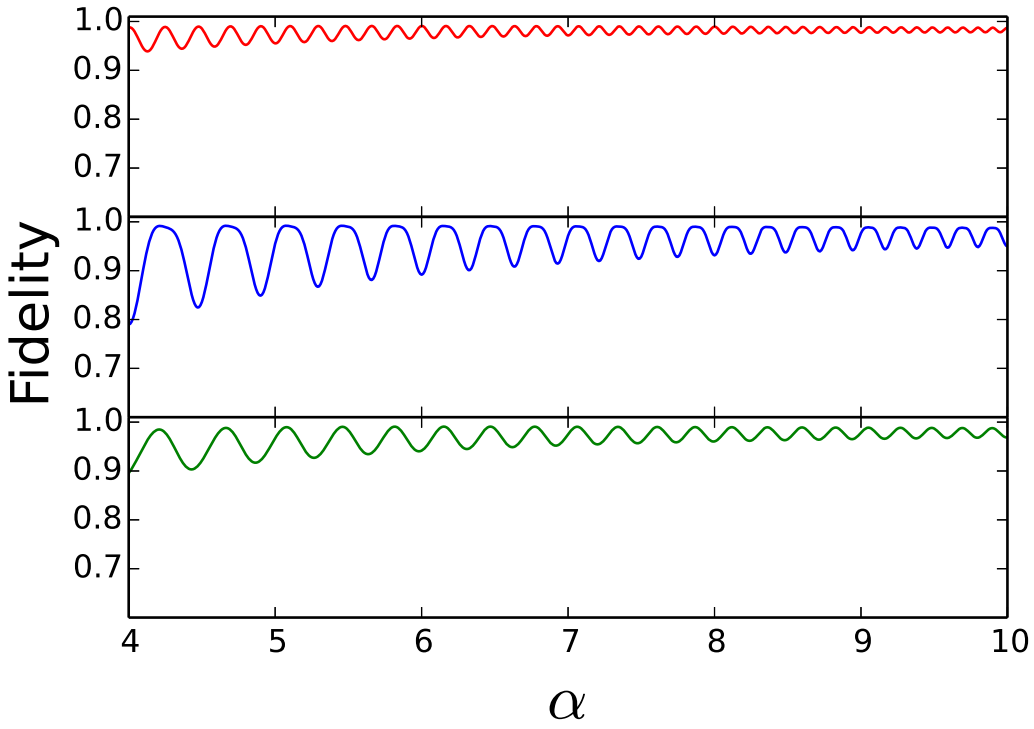

Figure 5

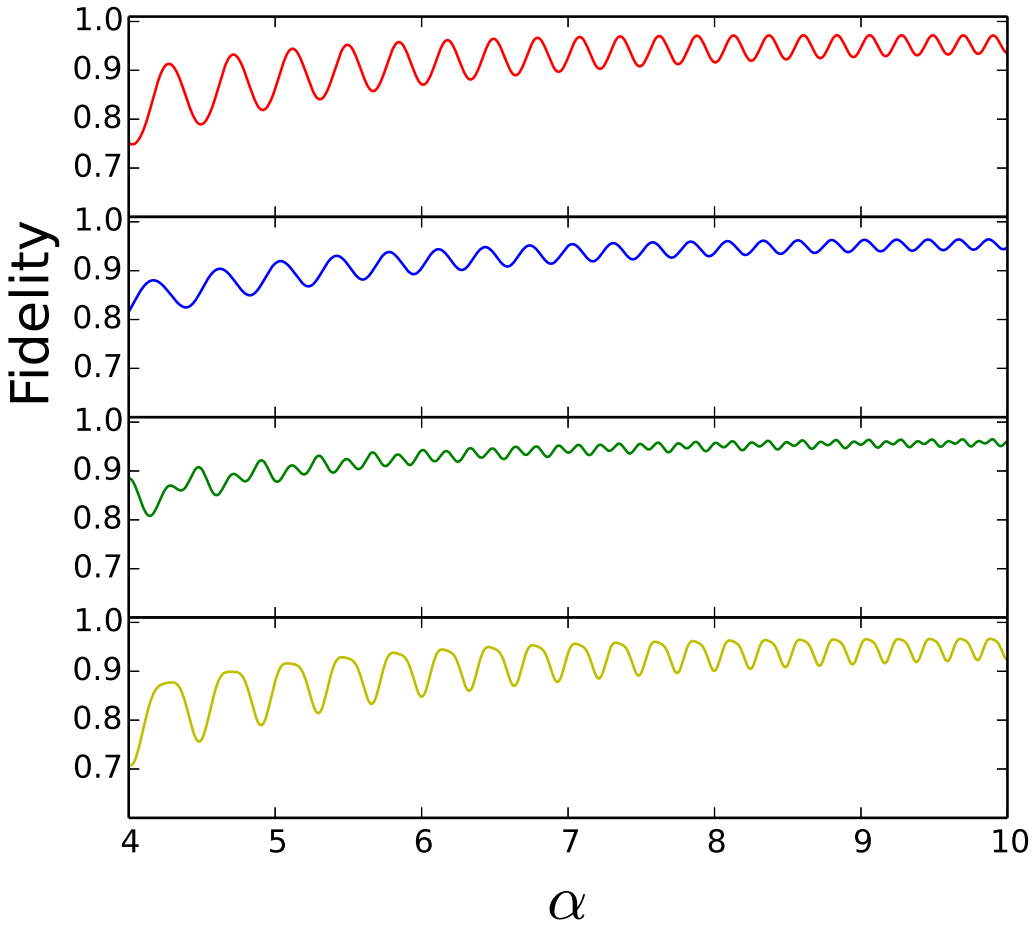

Supplementary Information

When the inter-cavity crosstalk between resonators are considered, the Hamiltonian (1) is modified as follows

$$\begin{aligned} H_{\rm I}' &= \sum_{j=1}^{2}\left(g_j e^{i\Delta_j t}\hat{a}_j\sigma^+ + \mu_j e^{i\Delta_j t}\hat{b}_j\sigma^+ + {\rm H.c.}\right) \\ &\quad + \left(g_{a_1a_2}e^{i\delta t}a_1a_2^\dagger + g_{a_1b_2}e^{i\delta t}a_1b_2^\dagger + {\rm H.c.}\right) \\ &\quad + \left(g_{a_2b_1}e^{-i\delta t}a_2b_1^\dagger + g_{b_2b_1}e^{-i\delta t}b_2b_1^\dagger + {\rm H.c.}\right) \\ &\quad + \left(g_{a_1b_1}a_1b_1^\dagger + g_{a_2b_2}a_2b_2^\dagger + {\rm H.c.}\right), \end{aligned} \tag{S1}$$

where the terms in the last three lines represent the inter-cavity crosstalk between any two resonators, with the coupling constants ($g_{a_1a_2}, g_{a_1b_2}, g_{a_2b_1}, g_{b_2b_1}, g_{a_1b_1}, g_{a_2b_2}$) and detuning $\delta = \omega_{a_2} - \omega_{a_1} = \omega_{b_2} - \omega_{a_1} = \omega_{a_2} - \omega_{b_1} = \omega_{b_2} - \omega_{b_1}$ of the two associated resonators, due to $\omega_{a_1} = \omega_{b_1}$ and $\omega_{a_2} = \omega_{b_2}$.

The numerical simulation is performed by solving the master equation (10), with the Hamiltonian $H_{\rm I}$ there replaced by $H_{\rm I}'$. For simplicity, we set $g_{a_1a_2} = g_{a_1b_2} = g_{a_2b_1} = g_{b_2b_1} = g_{a_1b_1} = g_{a_2b_2} \equiv 0.01g$ (a conservative consideration for weak direct inter-resonator crosstalks). In our numerical simulation, the detuning setting $\Delta_1 = -\Delta_2 = \Delta,$ the coupler-resonator coupling constants $g_1 = \mu_1 = g_2 = \mu_2 = g = 2\pi \times 100$ MHz, the resonator photon lifetime, and the decoherence time of the coupler are the same as those used for Figs. (4) and (5) of the main text. The operational fidelity as a function of the dimensionless detuning $\alpha \equiv \Delta/g$ in the range of $4 \leq \alpha \leq 10$ for Bell state transfer and exchange are plotted in Figs. S1 and S2, respectively. Compared Fig. S1 (S2)

with Fig. 4 (5) of the main tex, it can be seen that the high fidelity is hardly affected by weak direct inter-resonator crosstalks for both Bell state transfer and exchange.

Figure S1: Fidelity versus α for the Bell-state transfer. The curves in (a), (b), and (c) correspond to transferring the Bell states $|\psi^+\rangle$, $|\psi^-\rangle$, and $|\phi^\pm\rangle$, respectively. Here, the red curves are plotted without considering the inter-resonator crosstalks, while the blue ones take the weak inter-resonator crosstalks into account.

Figure S2: Fidelity versus α for the Bell-state exchange. The curves in (a), (b), (c), and (d) correspond to exchanging the Bell states, i.e, $|\psi^+\rangle$ with $|\psi^-\rangle$, $|\phi^+\rangle$ with $|\phi^-\rangle$, $|\phi^\pm\rangle$ with $|\psi^+\rangle$, and $|\phi^\pm\rangle$ with $|\psi^-\rangle$, respectively. Here, the red curves are plotted without considering the inter-resonator crosstalks, while the blue ones are plotted by taking the weak inter-resonator crosstalks into account.

Figure S1

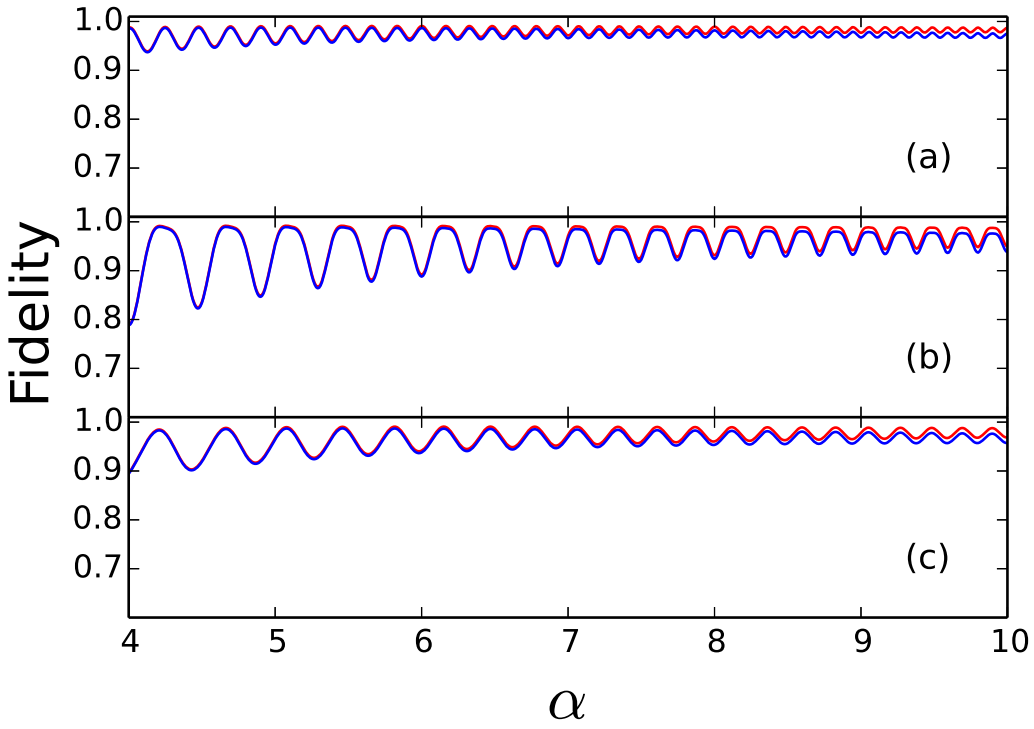

Figure S2